Interaction between plates in a polymer melt

ten Brinke, Gerrit ; Ausserre, Dominique; Hadziioannou, Georges

Published in:
The Journal of Chemical Physics

DOI:
10.1063/1.454823

Publication date:
1988

Interaction between plates in a polymer melt

Gerrit ten Brinke,[a] Dominique Ausserre,[b] and Georges Hadziioannou
IBM Research Division, Almaden Research Center, San Jose, California 95120-6099

(Received 2 June 1988; accepted 15 June 1988)

The effect of confining a polymer melt between two parallel plates has been investigated using Monte Carlo simulations. As soon as the distance between the plates becomes comparable to twice the radius of gyration of the polymer molecules in the bulk, the shape of all molecules is affected. Reducing the separation even more reduces the actual number of deformed molecules while the remaining molecules become on the average more deformed. The deformation of the molecules is due to those sections which are very near one of the two plates. The excess number of bonds parallel to the plates with respect to the bulk isotropic contribution is nearly independent of the distance between the plates. The correlation length is estimated to be of the order of the lattice spacing. All observations are in agreement with the predictions of de Gennes that no long-range force between plates in a melt should exist.

INTRODUCTION

The effect of a hard wall on the shape of polymer molecules in the melt was first studied by Helfand and coworkers.[1,2] A significant bond anisotropy due to the condition of incompressibility was predicted. In the bulk unperturbed by the presence of hard walls, polymer coils satisfy Gaussian statistics, first predicted by Flory[3–5] and subsequently confirmed by neutron scattering experiments.[6,7] Near a solid wall, it is impossible to satisfy the space filling condition unless the molecules are strongly deformed. Similar problems are encountered in the case of semicrystalline polymers. Here, space filling considerations imply that a large fraction of molecules emerging from the crystalline phase have to reenter adjacently.[8–10]

Besides analytic methods, Monte Carlo simulations have become increasingly important for our understanding of the behavior of polymer molecules in the melt.[11–16] Most studies concern the dynamics and, in particular, the validity of the reptation concept,[11–14] but in recent papers, the static properties of polymer molecules in thin films were also investigated.[16] Furthermore, the interactions between plates in a polymer solution have been the focus of much theoretical and experimental work.[16–24] Here, important parameters are the interaction between the molecules and the plates and the architecture of the polymers. The case of a polymer solution differs from a polymer melt in the sense that the polymer concentration of the solution between the plates can adjust itself to the distance between the plates. As shown, for instance, by Feigin and Napper,[25] an approach of two neutral plates to closer than twice the root-mean-square end-to-end distance of the polymers results in a significant reduction of the polymer concentration. On an even closer approach, the polymer density reduces effectively to zero. In the case of a polymer melt, this is obviously impossible, and the polymer coils will become more and more deformed.

As far as the interaction between two neutral plates in a polymer melt is concerned, two opposing effects have to be taken into account, once the distance between the plates becomes comparable to twice the root-mean-square radius of gyration. Suppose for a given distance D, there are n chains between the plates. Let ΔS_1 denote the average entropy per chain difference between a chain confined between the plates and a "free" chain. Then, $\Delta S = n\Delta S_1$ where n and ΔS_1 are functions of D, and hence

$$d\Delta S/dD = dn/dD \cdot \Delta S_1 + n d\Delta S_1/dD. \quad (1)$$

Let ρ be the polymer density and Σ the surface per plate. Then

$$d\Delta S/dD = \rho\Sigma(\Delta S_1 + D d\Delta S_1/dD). \quad (2)$$

If a chain satisfies Gaussian statistics, Casassa[26] showed already $\Delta S_1 \sim -D^{-2}$. Since chains in a melt also satisfy Gaussian statistics, this seems to imply that

$$d\Delta S/dD \simeq \rho\Sigma(-D^{-2} + 2D^{-2}) = \rho\Sigma D^{-2} \quad (3)$$

and consequently, a repulsive force between the plates would exist. However, this argument is wrong for the simple reason that for a single chain, the interaction with the wall is not screened out as it is in melt. de Gennes already predicted[27] that in the latter case no long-range interaction should be present. This conclusion remains valid if short-range repulsive or attractive interactions between the plates and the chains are present. For two neutral plates, the results of our Monte Carlo calculations are in good agreement with de Gennes predictions. The long-range repulsive forces observed experimentally[28,29] for the case where absorption is present may be due to the fact that those chains which are in direct contact with the plates are pinned at the contact points.[27] So the experimental conditions[28,29] are not directly comparable with our calculations since the polymer chains interact very strongly with the wall.

THE MODEL

To simulate the behavior of polymer molecules in a melt confined between two parallel plates, dynamic Monte Carlo calculations were performed. A cubic lattice model was used because of its simplicity with respect to the boundary condi-

[a] Permanent address: Department of Polymer Chemistry, University of Groningen, Nijenborgh 16, 9747 AG, Groningen, The Netherlands.
[b] Permanent address: Physique de la Matière Condensée, Collège de France, 11, Place Marcelin, Berthelot, 75231 Paris Cedex 05, France.

 0021-9606/88/194374-07$02.10

tions. The plates were situated at $z = 1$ and $z = L$, where L is varied between 2 and 20. During the simulations, the chains are not allowed to cross these planes. In the two other directions, periodical boundary conditions were imposed. The periodical boundaries were located at $x = 1$, $x = 40$ and $y = 1$, $y = 40$. In all cases, the polymer concentration was $\phi = 0.8$, implying that 20% of all lattice sites remained empty, because every lattice site can be occupied by at most one polymer bead. This choice resulted from a compromise between two requirements. The model should represent the melt situation rather closely but at the same time have a sufficiently high success rate for the elementary motion attempts to be introduced. The limits put on the polymer concentration by the last requirement have been discussed by Kolinski *et al.*[30] for a diamond lattice model.

The use of cubic lattice models and Monte Carlo calculations for the study of static and dynamic properties of polymer molecules originates from Verdier and Stockmayer.[31] In a modified form, it has been applied to a variety of problems by Kovac and co-workers.[32–35] Our simulation method essentially combines the procedure introduced by Kolinski *et al.*[30] with the elementary bead motions used by Kovac *et al.*[32] The general features will be described briefly below. For more details, the reader is referred to the original papers.

In order to reduce the computing time, we follow Kolinski *et al.*[30] by growing and equilibrating chains simultaneously. The procedure starts by placing the first bead of all chains randomly in a suitable chosen subvolume of the total volume defined by the boundary conditions. Next, the subvolume is scaled up to the total volume and the coordinates of the beads are multiplied accordingly. In this way, severe clustering of the starting beads is avoided. Then the growing of the chains starts by adding beads to either end of a randomly chosen chain. Once the chosen chain happens to consist of five or more beads, growing and equilibrating start to compete. Somewhat arbitrarily, both possibilities are given equal probabilities. The equilibrating step always consists of a reptation step attempt followed by an elementary bead jump attempt. The reptation step, first introduced by Wall and Mandel,[36] consists of selecting a chain end at random, removing the corresponding end bead and adding it in an arbitrary fashion to the other end of the chain (Fig. 1). For the elementary bead jump, a distinction is made between an end bead and an internal bead. Whether an end-bead jump or an internal-bead jump is tried is again determined randomly. Also, which end bead in the first case or which internal bead in the second case is decided randomly. The possible jumps have been described thoroughly by Gurler *et al.*[32] The end-bead jump is a 90° flip and the internal bead jump is a normal bead motion, already used by Verdier and Stockmayer,[31] or a crankshaft motion (Fig. 2). The particular structure of the chain determines which, if any, internal bead jump is, in principle, possible. During the growing and equilibrating, double occupany of lattice sites as well as crossing the solid plates is forbidden. If any of these situations occurs, the attempt is rejected. If it happens during the growing step or the elementary bead jump attempt, the next cycle starts. A rejection of the reptation step is still followed by an elementary bead jump attempt. The procedure is summarized in Fig. 3.

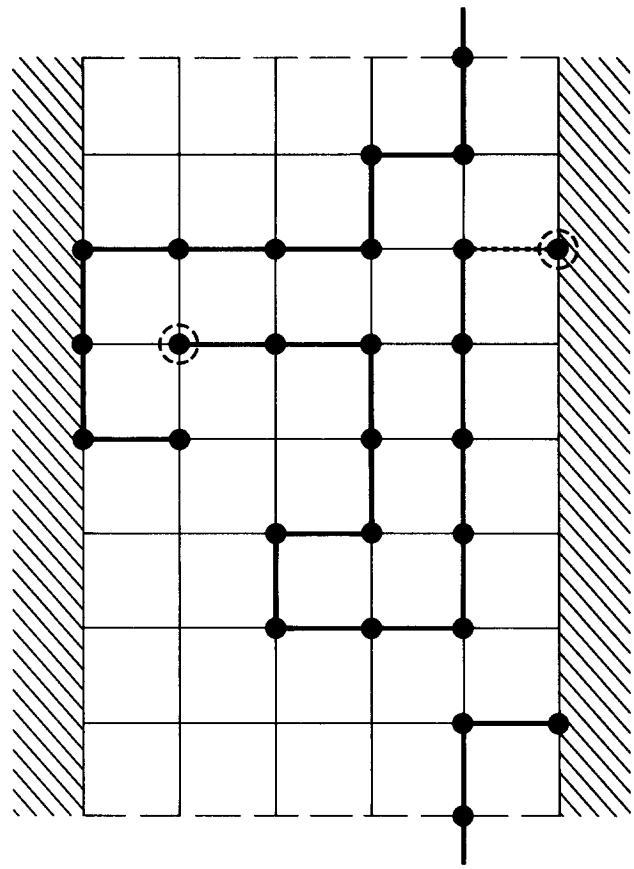

FIG. 1. Illustration of reptation step and boundary conditions.

Once all chains have reached their predescribed length, the growing stops completely. The equilibrating continues and after a number of additional cycles, usually of the order 10^6, the sampling starts. It consists of storing the configurations of the total system obtained from the starting configuration by a multiple of K cycles, K being the total number of beads in the system. In the cases considered here, the polymer concentration is 80%. The number of chains involved depends on the boundary conditions and the chain length. Three different chain lengths were considered, 40, 60, and 80

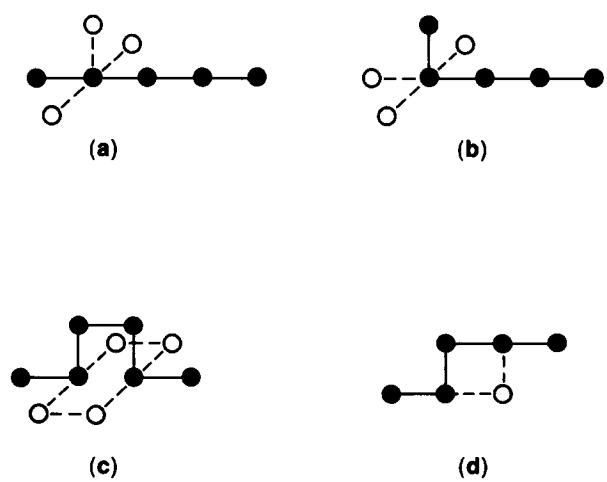

FIG. 2. Illustration of bead motions: (a) and (b) end-bead motion; (c) crankshaft motion; (d) normal bead motion.

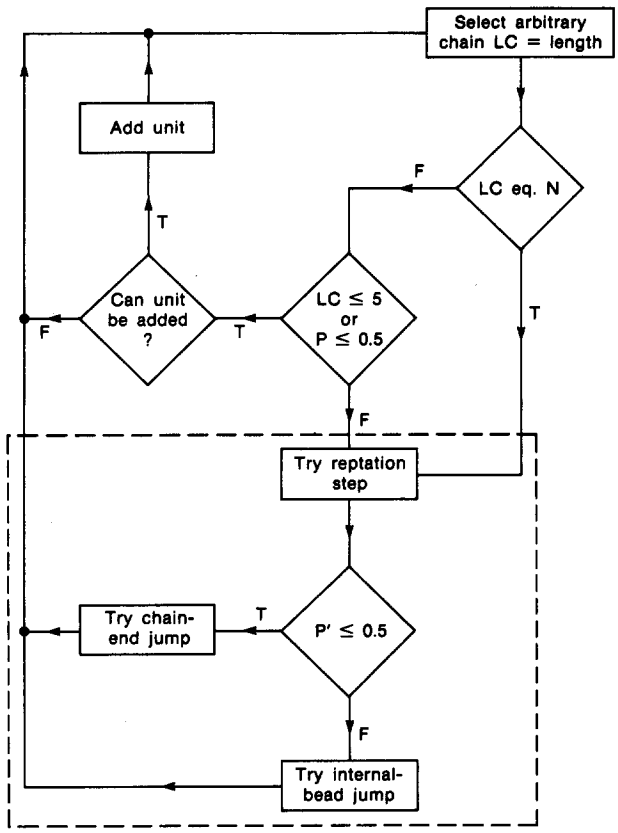

FIG. 3. Flow chart of the simulation procedure. P and P' are random numbers in between 0 and 1, LC is the instantaneous length expressed in number of beads. Dashed box represents the equilibration steps.

beads. For a fixed polymer concentration, K depends only on the boundary conditions. The number of cycles was of the order of 5×10^6. Of all attempts, reptation and bead jump, on the average 85% had to be rejected because of double occupancy or violation of the boundary conditions. This figure depended slightly on the distance between the parallel plates. To reduce the statistical error, in general, 5 to 10 independent runs were made. Averages were calculated, taking the symmetry of the system explicitly into account.

RESULTS AND DISCUSSION

Figure 4 shows the polymer bead density $\rho(z)$ as a function of z for chains of 60 beads. The plates are situated at $z=1$ and $z=20$. Since the overall density is 0.8, a slight depletion is present, which is essentially restricted to the density at the plates, an indication that the correlation length is of the order of the lattice spacing. A related quantity of interest is the end-bead density $\rho_e(z)$. In the case of a truly semidilute solution, the presence of a neutral wall leads to a strong depletion of the polymer density near the wall. There the end-segment density near the wall is also lower than in the bulk. However, the reduction in end-segment density is smaller than for the total segment density. The ratio of end segments to internal segments is enhanced near the wall. Precise calculations, in the mean-field limits, are available[37] for the particular case of a polydisperse semidilute system described by the well known $n\to0$ vector model.[38] In the case of a very concentrated solution considered here, the end-

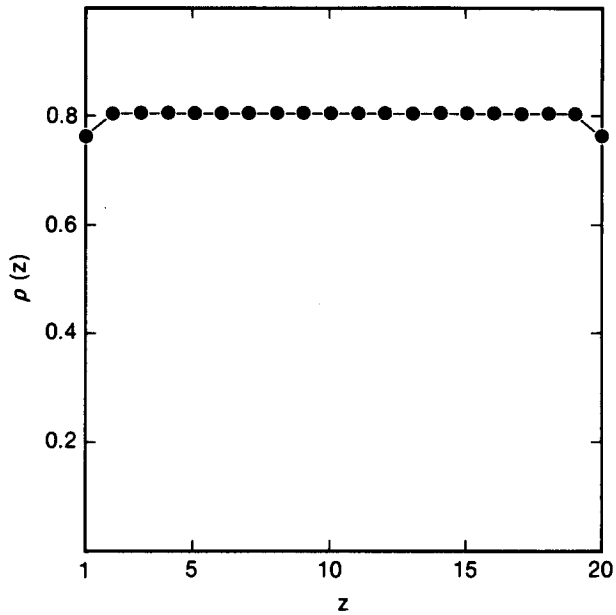

FIG. 4. Polymer bead density between plates situated at $z=1$ and $z=20$, $N=60$.

bead density near the wall is not only relatively enhanced, but also in absolute value larger than the average bulk value. Figures 5 and 6 show this for chains of 60 beads. The position of the second plate is at $z=20$ and $z=10$, respectively. The average end-bead density is given by $\bar\rho_e=0.0267$. To compensate for the enhanced end-bead density at the wall, the end-bead density is reduced over several lattice spacings. For the second plate at $z=10$, the end-bead density remains below $\bar\rho_e$ throughout the slit, whereas in the case of the second plate at $z=20$, it exceeds $\bar\rho_e$ again near the middle of the slit.

Table I(A) gives the end-bead density at the wall as a function of the number N of beads of the chains involved. In all cases, the second plate is at $z=20$. The number of end beads per surface unit in any plane parallel to the wall and far away from it (bulk) is given by

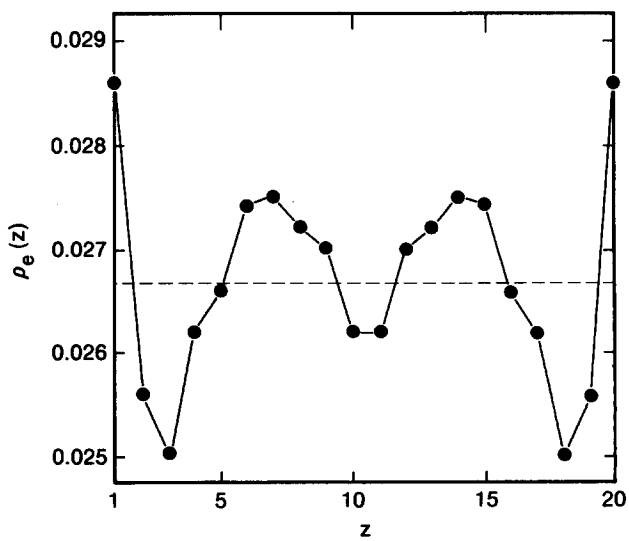

FIG. 5. End-bead density between plates situated at $z=1$ and $z=20$, $N=60$ and average bulk density $\bar\rho_e=0.0267$.

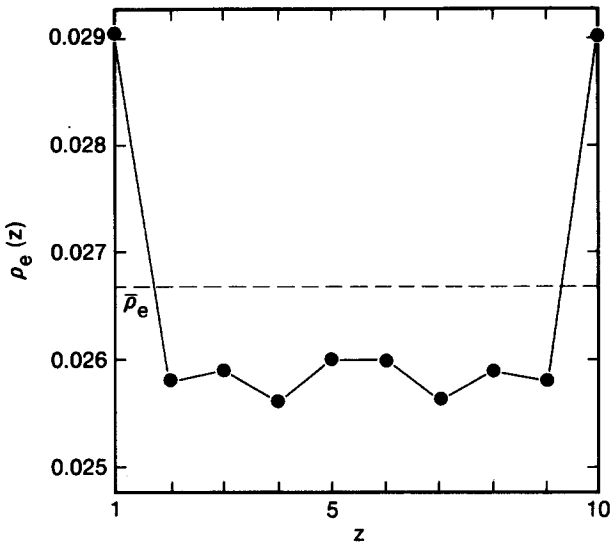

FIG. 6. End-bead density between plates situated at $z = 1$ and $z = 10$, $N = 60$ and average bulk density $\bar{\rho}_e = 0.0267$.

$$\rho_e(z) = \frac{2\phi}{Na^2}, \tag{4}$$

where $\phi = 0.8$ as before and a is the lattice spacing (equal to one). The data in Table I(A) show that at the surface

$$\rho_e(z = 1) = \frac{2\phi}{Na^2}\alpha, \tag{5}$$

where α is a constant given by

$$\alpha = 1.08 \pm 0.02. \tag{6}$$

The number of end beads at the wall is, therefore, proportional to the end-bead bulk concentration and the proportionality coefficient is slightly larger than 1.

All these features suggest an analogy with a weak adsorption of small molecules from a dilute system. We can, therefore, consider the bulk as a dilute solution of end beads in a solvent of non-end beads. The orientation of the solvent molecules at the wall gives rise to an attractive U_a for the solute. The partition coefficient between the surface and the bulk is thus given by

$$\rho_e(z = 1)/\bar{\rho}_e = \exp - (U_a/kT) \tag{7}$$

or writing $\rho_e(z = 1) = \bar{\rho}_e(1 + \Delta\rho_e/\bar{\rho}_e)$,

$$1 + \Delta\rho_e/\bar{\rho}_e = \exp - (U_a/kT). \tag{8}$$

TABLE I. End-bead density $\rho_e(z = 1)$.[a]

	N	$\rho_e(z = 1)$
(A) At the surface		
	40	0.0433 ± 0.0006
	60	0.0286 ± 0.0007
	80	0.0215 ± 0.0004
(B) At the surface as a function of L		
	6	0.0289 ± 0.0006
	8	0.0287 ± 0.0006
	10	0.0294 ± 0.0005
	20	0.0286 ± 0.0007

[a]Standard deviations based on five independent runs.

Since $\Delta\rho_e/\bar{\rho}_e \ll 1$,

$$U_a/kT = -\Delta\rho_e/\bar{\rho}_e = -(\alpha - 1). \tag{9}$$

The adsorption energy per end bead is independent of N. The surface energy contribution of the end beads should be proportional to the end-bead bulk concentration, i.e., proportional to N^{-1}.

Table I(B) contains $\rho_e(z = 1)$ as a function of the position L of the second plate for $N = 60$. The data show that U_a is independent of the distance D between the plates. As a consequence, the weak end-bead adsorption is of no significance as far as the interaction between the plates is concerned.

Figure 7 shows the distribution of the center of masses of the polymer molecules $\rho_{c.m.}(z_{c.m.})$ for chains of 60 beads and plates at $z = 1$ and $z = 20$. This is a discrete normalized distribution obtained by averaging over all chains with a center of mass in between z and $z + 1$, where z varies from 1 to 19. Near the plates, the center of mass density is strongly depressed, but this is compensated by two maxima. The positions of these maxima is determined by the chain lengths of the molecules. Later, we will give an estimation for the root-mean-square radius of gyration $\langle R_g^2\rangle^{1/2}$ of the polymer chains unperturbed by the presence of solid walls. It turns out that the distance between the plate and the nearest maximum is comparable to $\langle R_g^2\rangle^{1/2}$. This is also observed for the other chain lengths considered. In the middle between the plates, a plateau value for the center of mass density is found. Similar observations have been made by Madden[16] using a completely different simulation algorithm leading to a polydisperse sample. Very recently, these results were also obtained by Kumar, Vacatello, and Yoon[39] using off lattice calculations.

From here on, we will concentrate on the deformation of the polymer molecules. Figure 8 shows the number of bonds per molecule an $(z_{c.m.})$ which are parallel to the plates as a

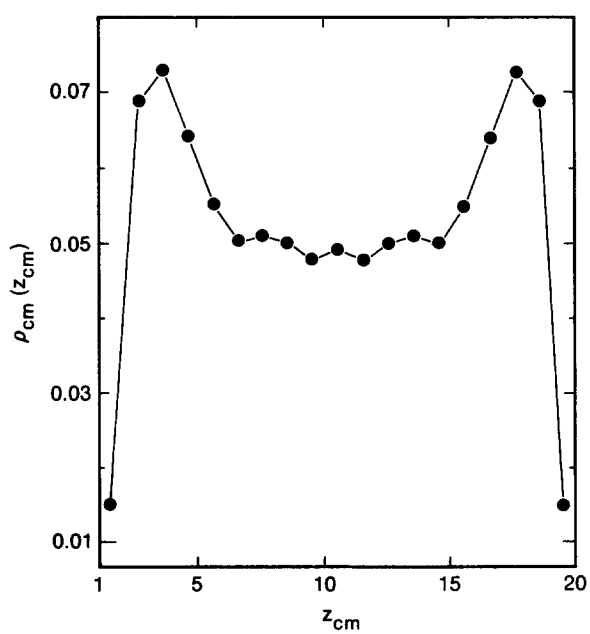

FIG. 7. Normalized center of mass density between plates situated at $z = 1$ and $z = 20$, $N = 60$.

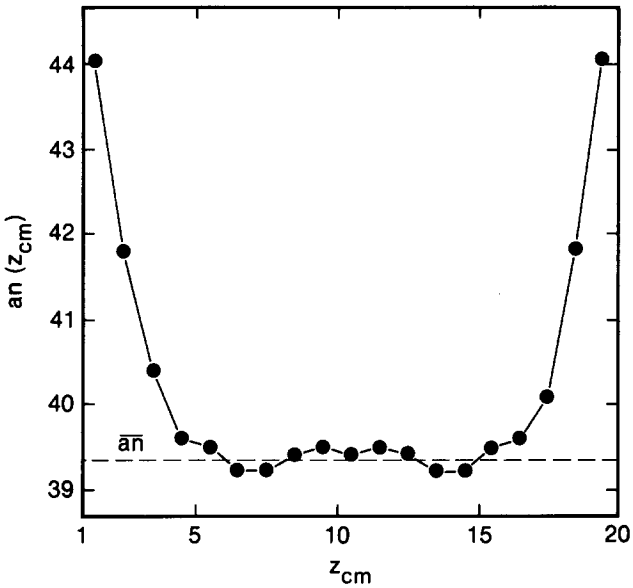

FIG. 8. Number of bonds $an(z_{c.m.})$ parallel to the plates as a function of the position of the center of mass. The plates are situated at $z = 1$ and $z = 20$, $N = 60$. $\overline{an} \simeq 39.3$ is the average bulk value.

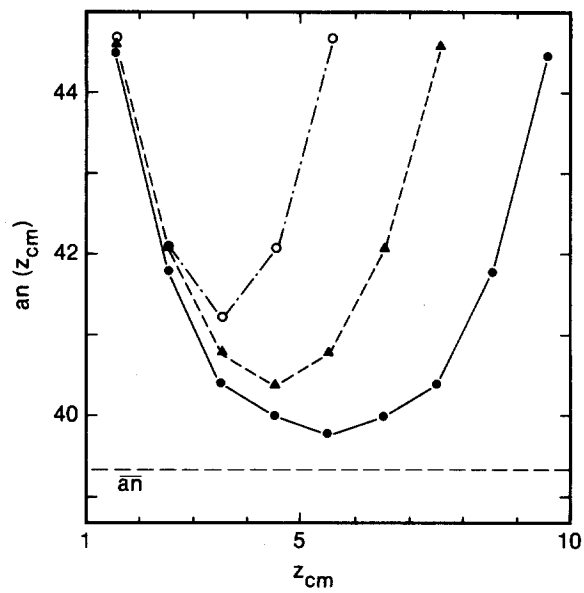

FIG. 9. Number of bonds $an(z_{c.m.})$ parallel to the plates as a function of the position of the center of mass. The first plate is at $z = 1$, $N = 60$. Second plate: (—), $z = 10$; (---)$z = 8$; (-·-·-), $z = 6$. $\overline{an} \simeq 39.3$ is the average bulk value.

function of the position $z_{c.m.}$ of the center of mass of the molecules. $an(z_{c.m.})$ is also a discrete distribution obtained by averaging over all chains with a center of mass inbetween z and $z + 1$. As before, z varies between 1 and D, D being the distance between the plates. The results in Fig. 8 are for $N = 60$ and the second plate located at $z = 20$ ($D = 19$). The average value $\overline{an}$ for molecules in the bulk is given by $2 \times 59/3 = 39.3$. As expected, the actual value of $an(z_{c.m.})$ exceeds $\overline{an}$ for those molecules having a center of mass sufficiently close to the plates. As will be demonstrated more clearly later, the deformation of the molecules is almost exclusively due to those sections of the molecules which are at or very near the plates. In agreement with this observation is the fact that only those molecules with a center of mass within a distance of the order of the unperturbed radius of gyration $\langle R_g^2 \rangle^{1/2}$ show a significant anisotropy. Near the middle of the slit, a plateau value is reached approximately equal to $\overline{an}$.

Figure 9 shows similar results for $an(z_{c.m.})$ with the second plate located at $z = 6$, 8, and 10, respectively. It shows that the anisotropy of those molecules which are sufficiently close to the first plate is not really affected by the approach of the second plate (and vice versa). This demonstrates again that the deformation is due to the chain sections located at or near the surface. For the same reason, the anisotropy of the molecules near the middle of the slit increases significantly once the interplate distance becomes smaller than twice the unperturbed radius of gyration.

We will now take a closer look at this deformation. The lattice contains L planes parallel to the plates where L includes the two plates. These planes are called horizontal. Let $n_\parallel$ denote the total number of horizontal bonds in the slit and $n_\perp$ the total number of vertical bonds. The fraction of horizontal bonds $F_\parallel$ is given by

$$F_\parallel = n_\parallel/(n_\parallel + n_\perp). \tag{10}$$

For a slit containing L horizontal planes, this becomes

$$F_\parallel = [2L/(3L - 1)]. \tag{11}$$

$F_\parallel$ deviates from the bulk value 2/3 because there is one more horizontal plane than there are layers in between the horizontal planes. $F_\parallel$ will be compared with the fraction of horizontal (or parallel) bonds per chain $\langle f_\parallel \rangle$ obtained by averaging over all chains in the slit. $\langle f_\parallel \rangle$ is defined in the following way:

$$\langle f_\parallel \rangle = \langle an(z_{c.m.}) \rangle/(N - 1), \tag{12}$$

where

$$\langle an(z_{c.m.}) \rangle = \sum_{z_{c.m.}} \rho_{c.m.}(z_{c.m.}) an(z_{c.m.}) \tag{13}$$

and $N - 1$ is the number of bonds per chain. Figure 10 shows $F_\parallel$ as well as $\langle f_\parallel \rangle$ as a function of L for $N = 40$, 60, and 80. For a given value of L, the values of $\langle f_\parallel \rangle$ for the three different values of N virtually coincide. The actual values are therefore also given in Table II. The close agreement between the theoretical values $F_\parallel$ and values $\langle f_\parallel \rangle$ found from our Monte Carlo calculations demonstrates that the average anisotropy is almost entirely due to those sections of the molecule that are at or very near the surface.

If both plates coincide ($L = 1$), a two-dimensional situation is obtained, all bonds of the remaining chains are horizontal and the excess number of horizontal bonds compared to the bulk case in just 1/3 of the total number of bonds. Our calculations show that the excess number of horizontal bonds of all the chains together in the slit is approximately independent of the interplate distance. This is, of course, also implied by the fact that $F_\parallel$ and $\langle f_\parallel \rangle$ are nearly equal. Helfand[1,2] and Theodoru[40] also observed that for polymers near a solid interface, the bond orientation deviates from isotropy only within a narrow interfacial region, alternating from layer to layer between a parallel and a perpendicular arrange-

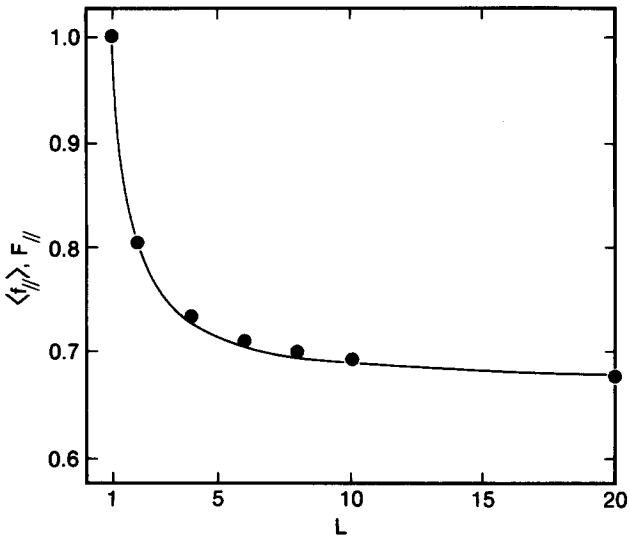

FIG. 10. Fraction of parallel bonds per molecule. Full line represents the calculated values of $F_{\parallel}$ following Eq. (11). Points correspond to the experimental values for indicated values of L. $N = 80$, 60, and 40 (cf. Table II).

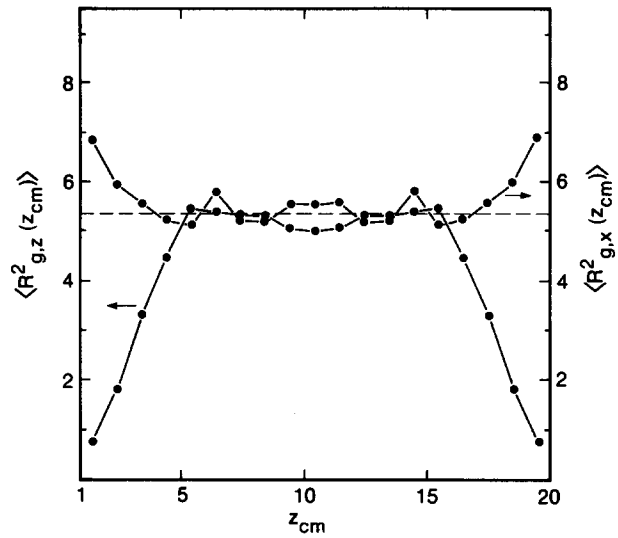

FIG. 11. Parallel (x) and orthogonal (z) component of the mean-square radius of gyration as a function of the position of the center of mass, $N = 60$ and second plate at $z = 20$. Dashed line corresponds to 1/3 $\langle R_g^2 \rangle$, where $\langle R_g^2 \rangle$ is the bulk value given in Table III.

ment with respect to the surface. Our calculations show that the excess number of horizontal bonds for the polymers in the slit is mainly determined by the geometry of the problem. The fact that this number is almost independent of L is a strong indication that the forces between the plates will be approximately zero. Bringing the plates closer together reduces the number of polymers in the slit, increases the average anisotropy per chain, but hardly affects the total excess of parallel segments per unit area. There is no reason to believe that a replacement of the neutral plates by adsorbing or repulsing plates will alter this conclusion.

Next, we consider the orthogonal and parallel component of the radius of gyration as a function of the position $z_{c.m.}$ of the center of mass. As before, an average was taken over all molecules with $z_{c.m.}$ in between z and $z + 1$, where z varies between 1 and D. Figure 11 shows the z and x component of the mean-square radius of gyration for $N = 60$ and $D = 19$. For molecules near the plates $\langle R^2_{g,x} \rangle$ is much larger than $\langle R^2_{g,z} \rangle$. Near the middle of the plates, a plateau value is reached. In the plateau regime, the parallel component of the mean-square radius of gyration is approximately equal to the orthogonal component. Figure 12 illustrates what happens if the distance between the plates is reduced. As in the case of $an(z_{c.m.})$, it is again observed that the chains with a center of mass sufficiently close to either plate are not really affected by this process.

In the foregoing, we mentioned a few times the unperturbed radius of gyration $\langle R_g^2 \rangle^{1/2}$. This quantity was estimated from the data available for the chain lengths of $N = 40$, 60, and 80 and plates situated at $z = 1$ and $z = 20$ in the following way. First, we notice that sufficiently far from the plates, the shape of the molecules is nearly isotropic (Figs. 11 and 12). $\langle R_g^2 \rangle^{1/2}$ was obtained by averaging over all molecules in this plateau regime. For the chain lengths considered $N = 40$, 60, and 80, respectively, this implied that all molecules with a center of mass within a distance of 3, 4, and 5, respectively, of either plates were disregarded. Then $\langle R_g^2 \rangle$ was obtained as the average over all remaining molecules $R^2_{g,x}(z_{c.m.}) + R^2_{g,y}(z_{c.m.}) + R^2_{g,z}(z_{c.m.})$. Table

TABLE II. Fraction of parallel bonds.

L	$F_{\parallel}$	$\langle f_{\parallel} \rangle, N = 40$	$\langle f_{\parallel} \rangle, N = 60$	$\langle f_{\parallel} \rangle, N = 80$
2	0.807	0.805	0.806	
4	0.727	0.734		
6	0.706	0.710	0.712	0.712
8	0.696	0.701	0.702	
10	0.690		0.692	0.690
20	0.678		0.676	0.679

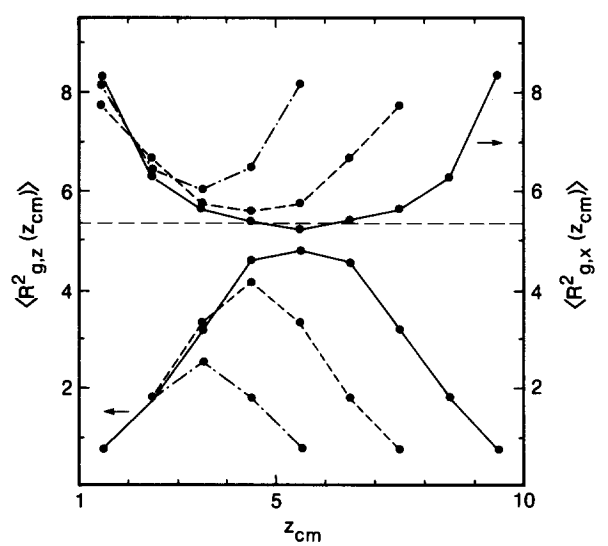

FIG. 12. Parallel (x) and orthogonal (z) component of the mean-square radius of gyration as a function of the position of the center of mass, $N = 60$ and first plate at $z = 1$. Second plate at: (—), $z = 10$; (---) $z = 8$; (-·-·-), $z = 6$. Dashed horizontal line corresponds to 1/3 $\langle R_g^2 \rangle$, where $\langle R_g^2 \rangle$ is the bulk value given in Table III.

TABLE III. Equilibrium dimensions of polymer chains at $\phi = 0.8$.[a]

N	$\langle R_g^2 \rangle$	$\langle R_g^2 \rangle / \langle R_g^2 \rangle_0$	$\langle R_g^2 \rangle / \langle R_g^2 \rangle_{\mathrm{NRRW}}$
40	10.56($\pm$0.10)	1.58($\pm$0.02)	1.12($\pm$0.01)
60	16.03($\pm$0.33)	1.60($\pm$0.03)	1.11($\pm$0.02)
80	21.89($\pm$0.41)	1.64($\pm$0.03)	1.12($\pm$0.02)

[a] Standard deviations based on five independent runs.

III contains the values obtained in this way together with the ratios $\langle R_g^2 \rangle / \langle R_g^2 \rangle_0$ and $\langle R_g^2 \rangle / \langle R_g^2 \rangle_{\mathrm{NRRW}}$, $\langle R_g^2 \rangle_0$ is the random flight value given by[41]

$$\langle R_g^2 \rangle_0 = \tfrac{1}{6}(N-1)(N+1)/N \tag{14}$$

and $\langle R_g^2 \rangle_{\mathrm{NRRW}}$ is the nonreversal random walk value given by[42]

$$\langle R_g^2 \rangle_{\mathrm{NRRW}} \simeq \tfrac{1}{4}(N-2)N/(N-1) - \tfrac{5}{16}(N-2)/(N-1). \tag{15}$$

The expected proportionality $\langle R_g^2 \rangle \sim (N-1)$ is reasonably satisfied. The values of $\langle R_g^2 \rangle / \langle R_g^2 \rangle_0$ are considerably smaller than the value of 1.8 found by Kolinski *et al.*[30] However, they considered the case of $\phi = 0.5$. Theoretically, the concentration dependence of the mean-square radius of gyration in the semidilute good solvent regime is given by[5,38]

$$\langle R_g^2 \rangle \sim \phi^{-0.25}. \tag{16}$$

Maybe somewhat fortuitously, this dependence corresponds precisely to the difference found. A comparison with a nonreversal random walk is more realistic. In agreement with the results of Ref. 43, the polymer coils are also somewhat swollen compared to Eq. (15). However, the functional dependence of N as given by this equation is very well satisfied by the data.

CONCLUSIONS

In this short paper, the properties of a confined polymer melt were discussed on the basis of Monte Carlo calculations. The approach of the two confining plates reduces the number of molecules in the slit. The anisotropy of the remaining molecules increases. However, the total excess number of parallel bonds compared to the bulk state is approximately independent of the interplate distance. It is primarily determined by the geometry of the system. These observations are in good agreement with the theoretical predictions of de Gennes concerning the absence of long-range interactions between parallel plates in a melt.

ACKNOWLEDGMENTS

We thank Dr. William Madden and Dr. Doros N. Theodorou for making their manuscripts available prior to publication. We are grateful for stimulating discussions with Dr. Sanat Kumar. G.t.B. acknowledges the financial support of IBM Netherlands and the hospitality of the staff of IBM Almaden Research Center, San Jose, California. D. A. acknowledges the financial support of IBM France and the hospitality of the staff of IBM Almaden Research Center, San Jose, California.

[1] E. Helfand, Macromolecules **9**, 307 (1976).
[2] T. A. Weber and E. Helfand, Macromolecules **9**, 311 (1976).
[3] P. J. Flory, J. Chem. Phys. **17**, 303 (1949).
[4] P. J. Flory, *Principles of Polymer Chemistry* (Cornell University, Ithaca, 1953).
[5] P. G. de Gennes, *Scaling Concepts in Polymer Physics* (Cornell University, Ithaca, 1979).
[6] J. P. Cotton, D. Decker, H. Benoit, B. Farnoux, J. Higgins, G. Jannink, R. Ober, C. Picot, and J. des Cloiseaux, Macromolecules **7**, 863 (1974).
[7] R. G. Kirste, W. A. Kruse, and K. Ibel, Polymer **16**, 120 (1975).
[8] F. C. Frank, Faraday Soc. Gen. Discuss. **68**, 7 (1979).
[9] E. A. DiMarzio and C. M. Gutman, Polymer **21**, 733 (1980).
[10] C. M. Guttman, E. A. DiMarzio, and J. D. Hoffman, Polymer **22**, 1466 (1981).
[11] A. Kolinski, J. Skolnick, and R. Yaris, J. Chem. Phys. **86**, 1567 (1987).
[12] A. Kolinski, J. Skolnick, and R. Yaris, J. Chem. Phys. **86**, 7164 (1987).
[13] J. Skolnick, A. Kolinski, and R. Yaris, Acc. Chem. Res. **20**, 350 (1987).
[14] K. Kremer, Macromolecules **16**, 632 (1983).
[15] M. L. Mansfield, J. Chem. Phys. **77**, 1554 (1982).
[16] W. G. Madden, J. Chem. Phys. **87**, 1405 (1987); **88**, 3934 (1988).
[17] J. Klein, Nature (London) **288**, 248 (1980).
[18] J. Klein, J. Chem. Soc. Faraday Trans. 1 **79**, 99 (1983).
[19] J. Klein and P. Pincus, Macromolecules **15**, 1129 (1982).
[20] J. Klein and P. Luckham, Nature (London) **308**, 836 (1984).
[21] P. G. de Gennes, Macromolecules **15**, 492 (1982).
[22] J. N. Israelachvili, M. Tirrell, J. Klein, and Y. Almog, Macromolecules **17**, 204 (1984).
[23] J. M. H. M. Scheutjens and G. J. Fleer, Macromolecules **18**, 1882 (1985).
[24] G. Hadziiaonnou, S. Patel, S. Granick, and M. Tirrell, J. Am. Chem. Soc. **108**, 2869 (1986).
[25] R. I. Feigin and D. H. Napper, J. Colloid. Interface Sci. **75**, 525 (1980).
[26] E. F. Casassa, J. Polym. Sci., Part B **5**, 773 (1967).
[27] P. G. de Gennes, C. R. Acad. Sci. Paris **305**, 1181 (1987).
[28] J.-P. Montfort and G. Hadziioannou, J. Chem. Phys. **88**, 7187 (1988).
[29] G. Hadziioannou, S. Hirz, and C. Frank (to be published).
[30] A. Kolinski, J. Skolnick, and R. Yaris, J. Chem. Phys. **84**, 1922 (1986).
[31] P. H. Verdier and W. H. Stockmayer, J. Chem. Phys. **36**, 227 (1962).
[32] M. T. Gurler, C. C. Crabb, D. M. Dahlin, and J. Kovac, Macromolecules **16**, 398 (1982).
[33] C. C. Crabb and J. Kovac, Macromolecules **18**, 1430 (1985).
[34] M. Dial, K. S. Crabb, C. C. Crabb, and J. Kovac, Macromolecules **18**, 2215 (1985).
[35] J. Naghizadeh and J. Kovac, J. Chem. Phys. **84**, 3559 (1986).
[36] F. T. Wall and F. Mandel, J. Chem. Phys. **63**, 4692 (1975).
[37] G. ten Brinke, Internal Report, available on request.
[38] M. Daoud, J. P. Coton, B. Farnour, G. Jannink, G. Sarma, H. Benoit, R. Duplessix, C. Picot, and P. G. de Gennes, Macromolecules **8**, 804 (1975).
[39] S. Kumar, M. Vacatello, and D. Yoon, J. Chem. Phys. (to be published).
[40] D. N. Theodorou, Macromolecules **21**, 1422 (1988).
[41] P. J. Flory, *Statistical Mechanics of Chain Molecules* (Intersciences, New York, 1969).
[42] C. Domb and M. E. Fisher, Proc. Cambridge Philos. Soc. **54**, 48 (1958).
[43] A. Sariban and K. Binder, Macromolecules **21**, 711 (1988).